PERGAMON

Available online at www.sciencedirect.com
SCIENCE DIRECT®

Vision Research 43 (2003) 2141–2153

Vision Research

www.elsevier.com/locate/visres

Grouping local directional signals into moving contours

Peter J. Bex *, Anita J. Simmers, Steven C. Dakin

Institute of Ophthalmology, 11-43 Bath Street, London EC1V 9EL, UK

Received 17 June 2002; received in revised form 26 February 2003

Abstract

We consider how local motion signals are combined to represent the movements of spatially extensive objects. A series of band-pass target dots, whose collective motion defined a moving contour, was positioned within a field of randomly moving noise dots. The visibility of the contours did not depend on the direction of movement relative to local contour orientation unless the contour was constrained to pass through fixation, suggesting that a previously reported advantage for collinear motion trajectories depends on the probability of detecting any of the target elements rather than the integrated contour. Contour visibility was invariant of the spatial frequency of the elements, but it did depend on the speed, number and spacing of elements defining it, as well as the angle and spatial frequency difference between adjacent elements. Local averaging of directional signals is not sufficient to explain these results. The visibility of these moving contours identifies narrow-band grouping processes that are sensitive to the shape defined by the directions of the elements forming the contour.

Keywords: Motion; Trajectory; Contour; Spatial frequency

1. Introduction

The underlying processes that support the integration of stationary structure across visual space have been widely investigated with contour detection tasks introduced by Field, Hayes, and Hess (1993). In these tasks, observers are required to detect a contour defined by a number of narrow-band elements that are embedded in a large array of similar, but randomly oriented elements. The fact that contours are quite visible even when adjacent contour elements are widely spaced, or when they differ greatly in orientation or phase, means that it is unlikely that contours are detected by conventional receptive fields (Hess & Dakin, 1997); instead the results suggest that the responses of local units are grouped/integrated in order to signal the presence of a contour. For static stimuli, the constraints on grouping are fairly well established: the visibility of contours increases with: the length and straightness of the path (Field et al., 1993; Mullen, Beaudot, & McIlhagga, 2000; Pettet, 1999), although closure of highly curved contours can increase visibility, (Kovacs & Julesz, 1993); with increased exposure duration (Roelfsema, Scholte, & Spekreijse, 1999); and with the similarity in the phase (Dakin & Hess, 1999; Hess & Dakin, 1999; Keeble & Hess, 1999) or spatial frequency (Dakin & Hess, 1998a, 1998b, 1999) of the elements defining the contour. Contours can also be integrated within and across depth with similar factors determining visibility (Hess & Field, 1995; Hess, Hayes, & Kingdom, 1997).

A number of recent studies have examined how temporal relationships among isolated elements can be used to detect stimulus structure. Some controversial results have suggested that asynchronous changes in target and noise onset/offset (Usher & Donnelly, 1998) or synchronous change in target direction (Lee & Blake, 1999) in the absence of any detectable spatial cues can be sufficient to define visible form. However, the reader is advised to see Dakin and Bex (2002) and Beaudot (2002) for alternative explanations of onset/offset asynchrony results and Farid and Adelson (2001) and Morgan and Castet (2002) for alternative explanations of direction change results.

Others have examined how the spatial organisation of *directional* signals affects the visibility of the structure they define. Hayes (2000) employed moving and flickering contour displays to examine whether the *physical* or *perceived* positional relationships among path elements

* Corresponding author. Tel.: +44-207-608-4015; fax: +44-207-608-6983.

E-mail address: p.bex@ucl.ac.uk (P.J. Bex).

0042-6989/03/$ - see front matter © 2003 Elsevier Ltd. All rights reserved.
doi:10.1016/S0042-6989(03)00329-8

determined contour linking. When the sinusoidal carrier of a Gabor patch is set in motion within its static Gaussian envelope, the apparent location of the whole Gabor is shifted in the direction of carrier motion (Devalois & Devalois, 1991). For contour stimuli, this produces a perceived shift in the location of elements away from the underlying contour they define, which for static patterns is known to reduce its visibility (Field et al., 1993). Therefore with moving contour stimuli, it is possible to align either the *physical* locations of the contour elements (but thereby misalign their perceived locations); or to align their *perceived* locations (but thereby misalign their physical locations). Hayes (2000) found that contours were most visible when the perceived locations of the micro-patterns were aligned to compensate for the illusory shift, but their physical locations were misaligned. This result suggests that models of early visual processing should consider the perceived as well as the topographical locations coded by early visual filters.

We have recently reported that moving contours (drifting sinusoidal carriers within stationary Gaussian envelopes) were much more visible than their stationary counterparts with little effect of speed (Bex, Simmers, & Dakin, 2001). We also found that large speed differences (up to 10 fold) between adjacent elements did not significantly impair the visibility of the underlying contour. Taken together, these results suggest that motion cues play a role in contour grouping and that the direction of element movement is more important than their absolute speeds. Contours defined by elements aligned perpendicular to the local orientation of the underlying path were more visible when moving than when static, but were never as visible as contours defined by elements aligned parallel to the underlying path. This result is perhaps unsurprising because parallel contours are more visible than perpendicular ones even in the absence of motion (Field et al., 1993). When this static orientation cue is removed through the use of noise carriers instead of sine-wave grating carriers drifting within static Gaussian windows, perpendicular paths can be more visible than parallel ones (Ledgeway & Hess, 2002). Similarly, detection thresholds for three aligned dots is greater when they move parallel to their mean orientation axis than perpendicular to it (Verghese, McKee, & Grzywacz, 2000). Both these results suggest that directional signals are preferentially integrated along the trajectory of motion.

Bex et al. (2001) and Ledgeway and Hess (2002) examined the visibility of moving contours composed of drifting carriers within static Gaussian windows; the contours themselves did not move. Verghese et al. (2000) examined the visibility of contours that did move, but only employed dot triplets that defined short, straight contours. In the present manuscript, we examine how the organisation of local directional signals determines the visibility of spatial structure defined by motion with contours of variable length and curvature that moved through the display. We also examine the spatial frequency selectivity of the underlying motion grouping processes with band-pass filtered elements of variable spatial frequency.

2. Methods

The observers were the three authors, all of whom had normal or corrected visual acuity and were experienced in contour detection tasks. Stimuli were generated on a Macintosh G4 computer with software adapted from the VideoToolbox routines (Pelli, 1997) and were displayed on a LaCie Electron22 monitor in greyscale at a frame rate of 75 Hz and a mean luminance of 50 cd/m^2. The luminance of the display was linearised with pseudo-12 bit resolution (Pelli & Zhang, 1991) in monochrome and calibrated with a Minolta photometer. Images were presented in greyscale by amplifying and sending the same 12-bit monochrome signal to all RGB guns of the display. The display measured 34.6 cm horizontally (832 pixels), 26 cm vertically (624 pixels), and was 57 cm from the observer, in a dark room.

2.1. Stimuli

Stimuli were composed of dot elements that were digitally filtered (Press, Teukolsky, Vetterling, & Flannery, 1992) with logarithmic exponential filters. These filters have the advantage of shorter tails than Laplacian of Gaussian filters and are defined in the Fourier domain by:

$$A(f) = \exp\left(-\frac{\left|\ln(f/F_{\text{peak}})\right|^3 \ln 2}{(b_{0.5} \ln 2)^3} \right) \quad (1)$$

where F_{peak} specifies the peak frequency and $b_{0.5}$ the half bandwidth of the filter in octaves. We used three centre frequencies: $F_{\text{peak}} = 1.5$, 3 or 6 c/deg, the full bandwidth in all cases was one octave. The RMS contrast of elements was matched which approximately equates their visibility and apparent contrast (Moulden, Kingdom, & Gatley, 1990). Stimuli were composed of multiple filtered dots pseudo-randomly positioned in a 8 deg * 8 deg square region on the left or right of a central fixation cross. Each trial consisted of two 506 ms intervals ramped on and off with a raised cosine envelope over 40 ms. Each interval contained the same total number of elements, one interval contained a path plus a variable number of identical noise elements, the other interval contained only noise elements.

The construction of contours was the same as in many previous studies and is described in detail elsewhere (Field et al., 1993). In brief, the elements defining the contour were separated by a variable gap (from 0.3 to 1.6 deg) plus a random value between ±10% to

eliminate periodic cues to the presence of the path. The curvature of the contour was controlled by the path angle α, that determined the angle between adjacent elements (where $\alpha = 0$ deg defined a straight contour and curvature increased with α). The first element of the path was assigned a random orientation (between 0 and 360 deg), successive elements were placed at a location determined by the angle and spatial separation between adjacent elements. Unless under direct experimental manipulation, the standard parameters of the contour were as follows: each contour was composed of 6 elements, separated by 0.5 deg (±10%), with a contour angle (α) of 20 deg and the elements moved at a speed of 2.3 deg/s (1 pixel per video frame).

The complete contour was randomly positioned in the display and a variable number of noise elements were then randomly positioned in the display and assigned a random direction of motion that was constant throughout the trial. The motion of noise elements was the same as that of signal elements to prevent observers from exploiting spatio-temporal differences between target and noise elements which might be possible with, for example, random-walk noise elements whose motion energy cancels over time. Overlapping elements summed and elements that moved outside the display area were wrapped to the diametrically opposite point. The random interval contained the same number of elements, randomly positioned in the display and assigned random directions. An example of a typical frame from one of our movies is shown in Fig. 1a. As the contour is not visible unless the elements are set in motion, the elements defining the contour are plotted in reverse polarity in Fig. 1b for illustrative purposes only.

The observers' task was to fixate a central cross and to identify (with a button press) which of two intervals contained the contour. Auditory feedback followed incorrect responses. We employed a noise paradigm in which the number of noise elements was varied under the control of an adaptive QUEST staircase (Watson & Pelli, 1983) to establish the number of noise dots that were required for observers to discriminate the "contour + noise" interval from the "noise" interval on 75% trials. We adopted this procedure in preference to per-cent detection performance that is often used in path-finder experiments to avoid ceiling and floor performance effects. However, as in all signal:noise paradigms, this procedure varies the relative densities of target and noise elements. In the conventional signal:noise tasks, the total number of dots is held constant, and the number (i.e. density) of targets is reduced while that of noise elements is increased. This means that observers could in principle use density cues to detect the contour without ever detecting its motion. However, control experiments with static contours and the speed data in Fig. 5 show that observers were unable to detect contours unless they were moving and so were unable to utilise this potential cue. This paradigm has been used previously in studies of static (Moulden, 1994) and moving (Verghese et al., 2000) contours. In all Experiments, the levels of the parameter of interest (i.e. the parameter described along the x-axis of each graph) were randomly interleaved in a single run and each observer completed at least four runs for each condition in random order. The combined results over all runs for each observer were combined and fitted with a cumulative Normal function by least χ^2 fit, from which 75% threshold and 95% confidence intervals were estimated with standard methods (Press et al., 1992).

3. Experiment 1: direction of motion relative to the contour axis

We employed four types of contour element motion: three defined in relation to the *mean* contour orientation, and one in relation to the *local* contour orientation.

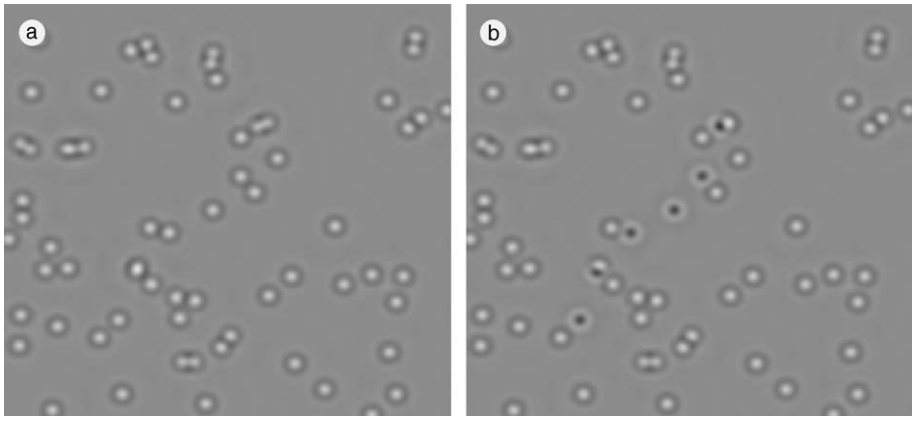

Fig. 1. Illustrations of a typical frame from the movie stimuli. (a) A random dot display containing a contour, as it would appear on screen. (b) All elements have been plotted in the same locations as in (a), but the six elements defining the contour have been plotted in reverse polarity so that they can be identified. In the same-polarity case, the contour is only visible when the elements defining it are set in motion.

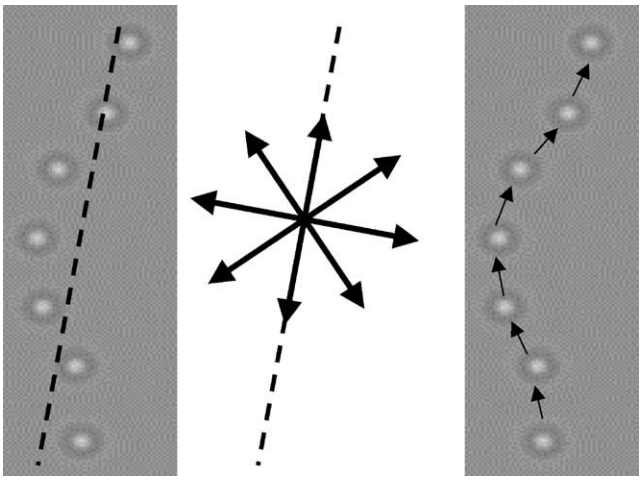

Fig. 2. Illustration of the potential directions in which contour elements could move. *Rigid motion*: left and centre, all elements moved relative to the mean orientation axis of the contour, shown by the broken line. Rigid motion occurred at 0, 45 or 90 deg relative to this axis, illustrated by the solid arrow in the centre panel and all contour elements moved at the same speed and direction. *Non-rigid motion*: right, elements moved directly towards the next element on the contour, indicated by the small arrows on the right panel, at the same speed, but necessarily in slightly different directions.

In the first three, contour elements moved in directions that were 0, 45 or 90 deg relative to the mean orientation axis of the contour (which randomly fell between 0 and 360 deg). Under these conditions the shape of the contour was unchanging and it moved *rigidly* through the display—see Fig. 2 left and centre panels. In the fourth condition, the elements moved directly towards the next element in the contour (the leading element headed towards imaginary elements that followed the same rules of contour construction but were not plotted). Thus the motion of the contour was *non-rigid* and the elements defining the contour could move in different directions within a single stimulus presentation and in different directions from one another.

Fig. 3 shows noise thresholds for each direction of rigid motion (at 0, 45 and 90 deg relative to the axis of the contour) and non-rigid motion. In all cases the path was composed of 6 elements that moved at a speed of 2.3 deg/s. The angle between adjacent elements along the contour (α) is shown in the caption, where 0 deg defined a straight contour and curvature increased with α. (see inset of Fig. 8 for examples). We observed only an advantage for straight over curved paths (we return to this in Section 4); in general there is little difference in the visibility of contours for any direction and under rigid or non-rigid contour motion.

4. Experiment 2: basic contour parameters

Given that under our experimental conditions, there was no effect of the direction of motion relative to the contour axis, we collected data with rigid contours that moved at 0 deg relative to the axis, and only observer PB collected a full set of data for non-rigid contours (filled circles in PB's data, all figures). The results in all cases were the same for rigid and non-rigid contours. The standard contour parameters were: 6 elements, each separated by 0.5 deg (± up to 10%), with an angular difference (α) of 20 deg and moving at 2.3 deg/s. These parameters were systematically manipulated in the following conditions. Fig. 4 shows that the visibility of a moving contour increases with the number of elements defining it which is broadly consistent with previous findings using static paths (Moulden, 1994). These data were well fitted by Weber functions, based on the assumption that the interval containing a contour is detected simply on the basis of the highest overall proportion of consistent directional signals, without any need for specialised contour linking operations. For two observers a good fit was obtained with a single Weber fraction for all spatial frequencies (PB 12% and SD 15%), the third observer (AS) was more sensitive to contours defined by elements with peak frequencies at 1.5 and 3 c/deg (14%) than to 6 c/deg (21%). The reduced sensitivity to higher spatial frequencies for this observer also occurs in her spatial frequency tuning data in Fig. 8.

Contours were generally more visible when they moved at higher speeds (Fig. 5). The performance of all subjects improved as contour speed increased from 0 to ~3.0 deg/s and then reached asymptote at higher speeds. This initially poor performance is unlikely to be due to a failure of local motion detectors to saturate within the stimulus presentation period because we observed little systematic influence of contour element spatial frequency as a function of speed. This shows that it is the speed of the elements and not their temporal frequency that determines the shape of this function.

Fig. 6 shows that, unsurprisingly, the visibility of moving contours increases with the proximity of adjacent contour elements. Data are plotted in Fig. 6A as a function of the physical spacing between elements, and in Fig. 6B as a function of the number of wavelengths of the peak frequency of the elements. Comparison between the figures shows that the data superimpose when plotted as a function of the physical spacing between the elements, even though this relative spacing increases with the centre frequency of the elements. This is quite unlike the data for static stimuli, in which spacing effects on contour visibility scale with the wavelength of the Gabor micro-pattern (Kovacs & Julesz, 1993). We return to this point in the discussion of spatial frequency tuning below.

The size of elements increases with wavelength so that, for a fixed display size, the *coverage* is greater for low centre frequency elements than for high (note that the density of the elements—# elements per unit area—is invariant of centre frequency). This means that the

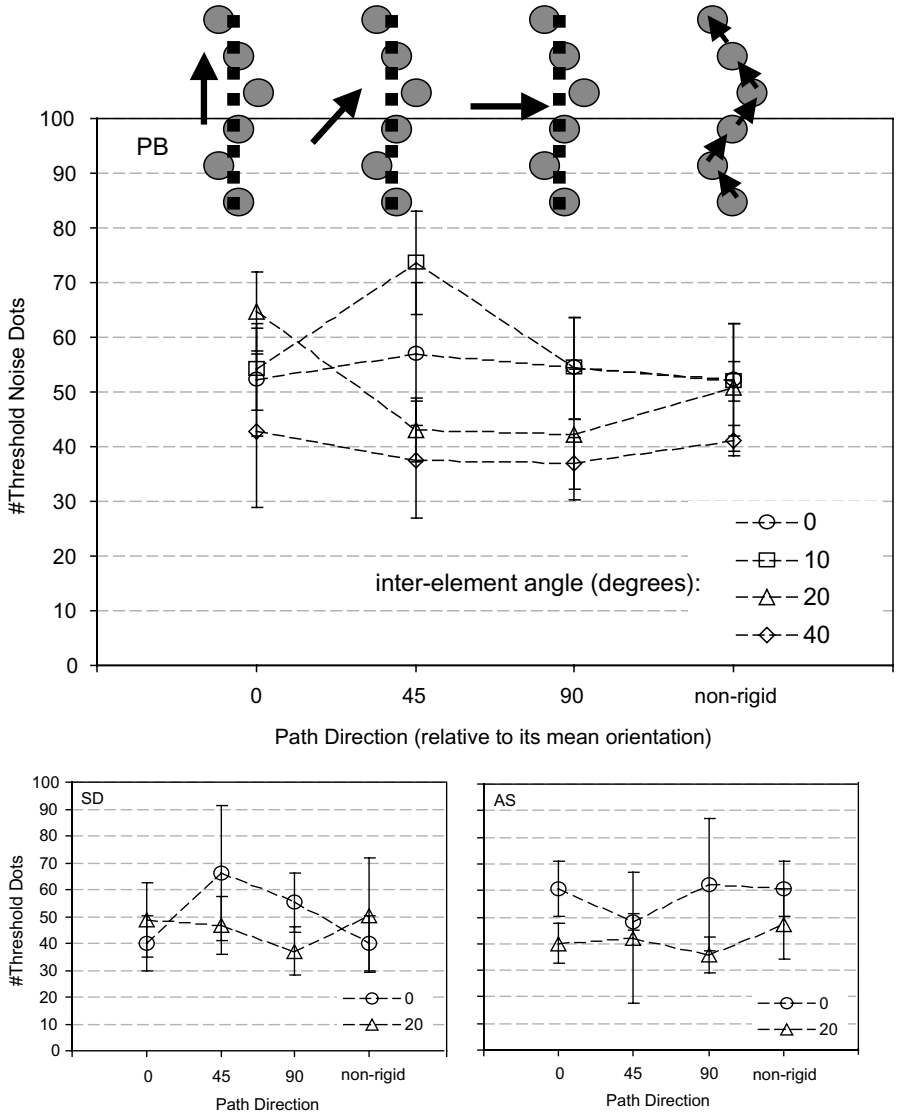

Fig. 3. Contour visibility as a function of the direction of motion of the elements defining it. The direction of movement of the six elements defining the contour is shown on the *x*-axis and is illustrated by the caption, the angle between adjacent contour elements (α) is shown in the legend. The data show the number of noise elements producing 75% correct discrimination of an interval containing a contour from an interval containing only noise elements. Error bars show 95% confidence intervals.

probability of part of a noise element falling between signal elements is greater for elements with low centre spatial frequency. In order to address this concern, observer SD collected a full set of data with the medium spatial frequency elements at double the viewing distance so they assumed a peak spatial frequency of 6 c/deg in a 4 deg stimulus region (filled triangles, all figures for SD). Under these viewing conditions, the results were identical in all cases. This is consistent with similar effects observed in static contour stimuli in which performance is approximately invariant of stimulus scaling (Hess & Dakin, 1997) and suggests that contour linking failures are related to density limitations where intrusions of noise elements in the line of the contour limit performance. Fig. 7 shows that the visibility of moving contours decreases at high curvature, but by no means as drastically as for static contour images (Field et al., 1993).

5. Experiment 3: spatial frequency selectivity

The results of Experiments 1 and 2 show remarkable invariance of contour visibility as a function of the spatial frequency of the elements defining the contour, suggesting either a single underlying contour-linking mechanism that is broadly tuned for spatial frequency or parallel, narrowly-tuned mechanisms operating on the same principles. To discriminate these candidates, we measured the spatial frequency selectivity of contour

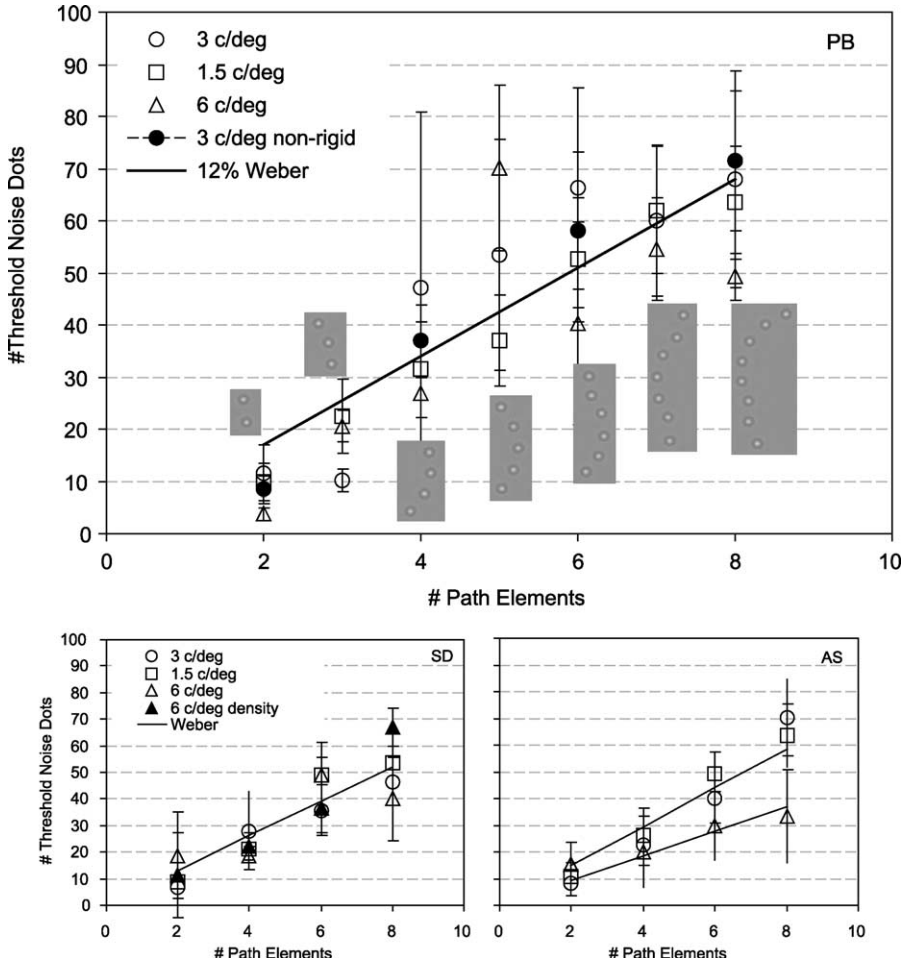

Fig. 4. Contour visibility as a function of its length. The data show the number of noise dots that produced 75% correct discrimination of an interval containing a contour and noise elements from an interval containing the same number of exclusively noise elements. The peak spatial frequency of the band-pass filtered elements is shown in the legend, the contour angle (α) was 20 deg, the spacing between adjacent contour elements was 0.5 deg and the contour elements moved rigidly at 0 deg relative to the axis of the path (open symbols) at 2.3 deg/s. Filled circles for observer PB show control observations for 3 c/deg elements moving non-rigidly. Filled triangles for observer SD show data for 6 c/deg control observations in which viewing distance was doubled. The number of elements defining the contour is shown on the *x*-axis. Error bars show 95% confidence intervals. The captions illustrate representative contours. The fits show Weber's law (least squares fitted, weighted by error bars).

integration. The visibility of a typical contour (composed of 6 elements, with a 20 deg angle and 0.5 deg ± 10% spacing between adjacent elements) was measured as a function of the spatial frequency difference between alternating elements. The centre frequency of alternate *target* elements along the contour was 3 c/deg, while the centre frequency of the remaining *fellow* elements varied from 1.5 to 6 c/deg in steps of 0.5 octaves. In a further (randomly interleaved) condition, 3 c/deg elements alternated in polarity between ON and OFF centre. See Fig. 9 insets for representative examples. Each noise element was randomly assigned the spatial frequency or contrast polarity of either the target or fellow elements.

Fig. 8 shows the spatial frequency tuning of motion contour integration. The data have been fitted with a log-Gaussian (which appears asymmetric on this linear *x*-axis). The peak spatial frequency of the function (PB 2.6; SD 3.1; AS 2.5 c/deg) is close to the target spatial frequency, indicating that best performance occurs when the spatial frequency of the target and fellow elements is similar. The estimated bandwidths (PB 2.6; SD 2.8; AS 2.2 octaves, ±1 SD) are broader than those reported for equivalent static stimuli (1.76 octaves for a 20 deg contour); (Dakin & Hess, 1998a, 1998b) Observer PB collected additional spatial frequency tuning data for paths with α set at 0 deg (straight) and 40 deg (highly curved)—see the captions in Fig. 7 for illustrations. Bandwidths under these conditions (0 deg = 2.9 and 40 deg = 3.2 octaves) did not systematically vary with contour angle as they do for static contours (Dakin & Hess, 1998a, 1998b). The visibility of contours composed of elements of alternating contrast polarity (same spatial frequency) was as high as for contours composed of elements of the same contrast polarity (Fig. 8, filled symbols).

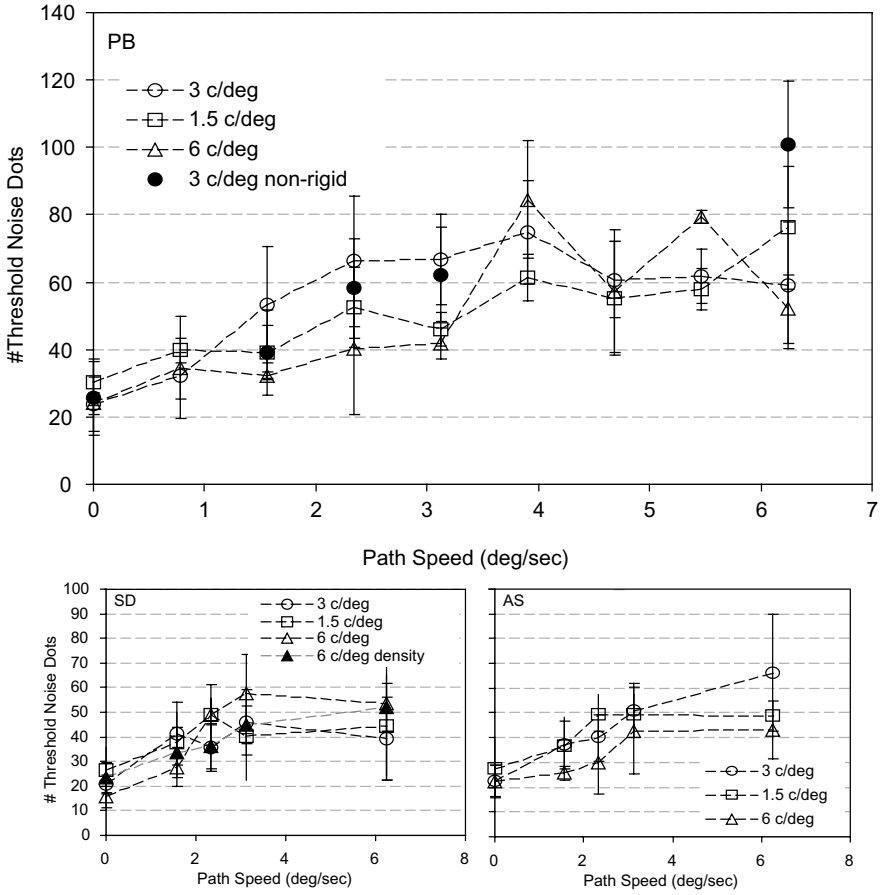

Fig. 5. Contour visibility as a function of speed. As Fig. 4 except that the number of elements defining the contour was fixed at 6 and the speed of elements was varied, as shown on the *x*-axis.

6. Discussion

We used band-pass random dot stimuli to examine how the spatial arrangement of local directional signals affects the visibility of the underlying structure they define. While Experiment 1 established that the direction of motion of the contour did not affect its visibility, Experiment 2 showed that contour visibility did increase with the number and proximity of the elements and with the speed and straightness of the contour. This pattern of results was the same for all spatial frequencies tested (1.5–6 c/deg) and signal:noise thresholds were approximately invariant of spatial frequency with our visibility-equated elements. We measured contour grouping across elements of differing spatial frequencies in Experiment 3 and found that the grouping process is broadly tuned for spatial frequency and not selective for contrast polarity.

6.1. Direction relative to the axis of the contour

We were surprised that the visibility of the contours was not affected by the direction of motion of the elements because a previous study using similar techniques has reported that contours moving at 0 deg relative to the contour-axis are more visible, at least for short (3 element), straight ($\alpha = 0$ deg) contours (Verghese et al., 2000). There were several differences between this study and our own that may account for this discrepancy. First, we used band-pass filtered elements, while Verghese et al. (2000) used 2 arcmin white dots that are broad in spatial frequency content. A second difference lies in the number of elements defining the contour; we used six, while they used three elements. Dr. Susanne McKee (personal communication) raised the possibly that the advantage of 0 deg directions could saturate for small numbers of path elements. To address these differences in curvature, spatial frequency and element number, we repeated our experiment with straight contours ($\alpha = 0$ deg) composed of varying numbers of broad-band Gaussian elements ($\sigma = 1.9$ arcmin) that were either white or black on a mean luminance background, to control for visual persistence and any phosphor persistence that might produce oriented smearing. The results are shown in Fig. 9. Unsurprisingly, the visibility of straight contours increased monotonically

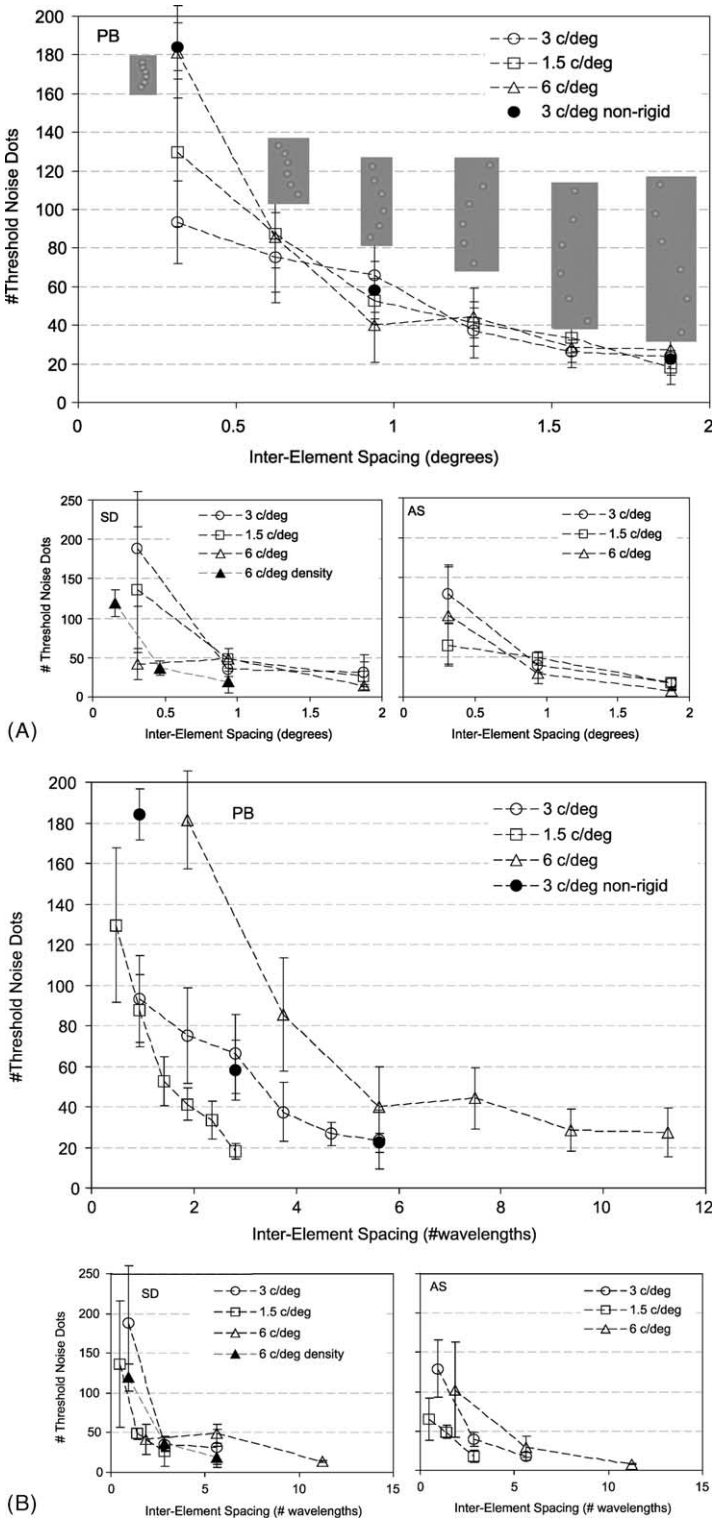

Fig. 6. Contour visibility as a function of inter-element separation. As Fig. 4 except that the number of elements defining the contour was fixed at 6 and the separation between adjacent contour elements was varied, as shown on the *x*-axis. (A) Inter-element spacing expressed as visual angle; (B) inter-element spacing expressed as multiples of the peak spatial frequency of the band-pass element.

with the number of elements defining them, as in Experiment 2. However, there was still no difference in the visibility of contours that moved parallel (circles) or orthogonal (squares) to the axis of the contour, for either positive (open symbols) or negative (filled symbols) polarity Gaussian elements. These results eliminate any of these variables as the source of the difference between studies.

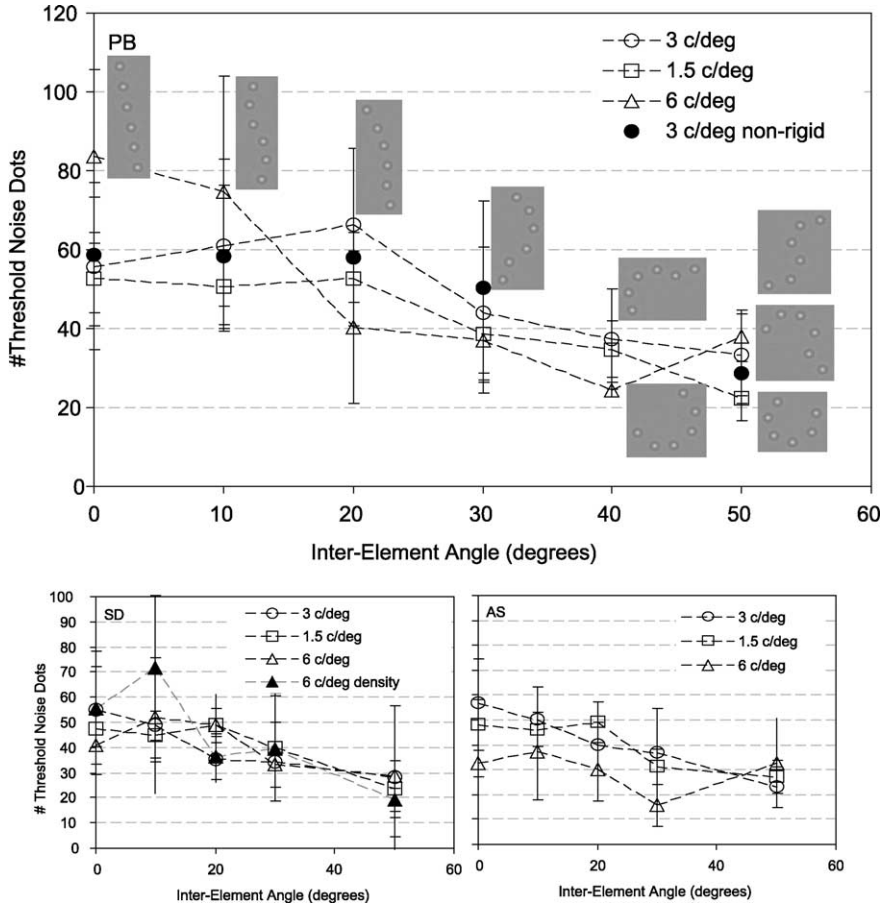

Fig. 7. Contour visibility as a function of inter-element angle. As Fig. 4 except that the number of elements defining the contour was fixed at 6 and the angle between adjacent contour elements (α) was varied, as shown on the x-axis.

Two further differences between studies concern the positioning of the target and the motion of the noise elements. In our study, the target could appear anywhere in the display whereas the centre element of the contours in the Verghese et al. (2000) study was constrained to pass within 0.25 deg of fixation in a 12.6 deg display. This region constituted less than 0.16% of the total display area, and so on average more than 600 dots are required over the entire display to add only one extra dot in this central area. Our stimulus is much less sensitive to such localised changes in dot number. The noise elements in the Verghese et al. (2000) study moved in random directions from frame to frame (random walk or Brownian motion), whereas our noise elements travelled in the same direction throughout the trial, which is known to affect the visibility of the target (Watamaniuk, McKee, & Grzywacz, 1995). These differences may explain the substantial differences between thresholds in the two studies; for three element contours, our thresholds were in the region of 30 noise elements, theirs were closer to 500. To reconcile these differences, we ran an additional control experiment with random walk noise (each noise element was assigned a new random direction every video frame) and we applied a positional constraint to the target: the centre element of a three element straight ($\alpha = 0$ deg) contour was forced to pass within 0.25, 0.5, 1 or 2 deg of fixation in separate runs. These data were collected in separate runs in which the observers knew the size of the constraint region in case this affected how observers distributed their attention. The results are shown in Fig. 10. We now confirm that targets moving parallel to their axis (0 deg) can be more resistant to noise than those moving perpendicular to it (90 deg), but this only happens only when the target is constrained to pass through foveal visual field. When this rule is relaxed, performance is the same for parallel and perpendicular targets. We speculate that the simplest explanation of the trajectory advantage is based on probability of detecting a coherently moving dot rather than sophisticated motion processing among moving dots. The foveal constraint on the centre element also affects the positions of the other contour elements. For parallel contours, fellow elements must also pass through fixation (one slightly before and one slightly after the centre element does), but this is not the case for fellow elements in perpendicular contours, which only sometimes pass the fovea. Owing to the higher acuity of foveal vision, this increases the probability that an

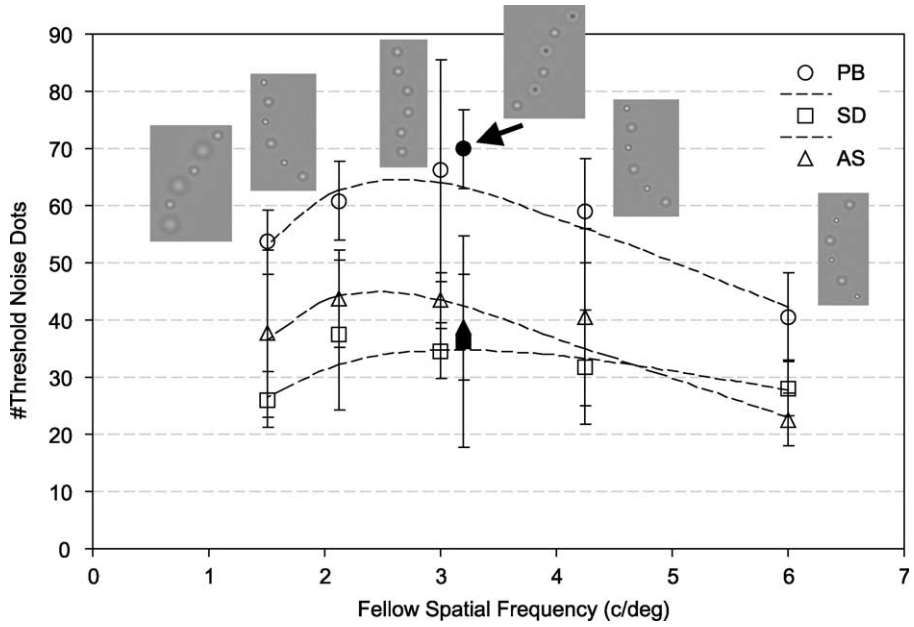

Fig. 8. Contour visibility as a function of the spatial frequency and contrast polarity difference between alternate contour elements. The spatial frequency of half the elements was fixed at 3 c/deg, the spatial frequency of the remaining interleaved elements is shown on the *x*-axis. The curves show log-Gaussian tuning functions (least squares fitted, weighted by error bars). Three observers, indicated by the legend. The filled symbol shows a single data point in which 3 c/deg elements were of alternating contrast polarity along the contour.

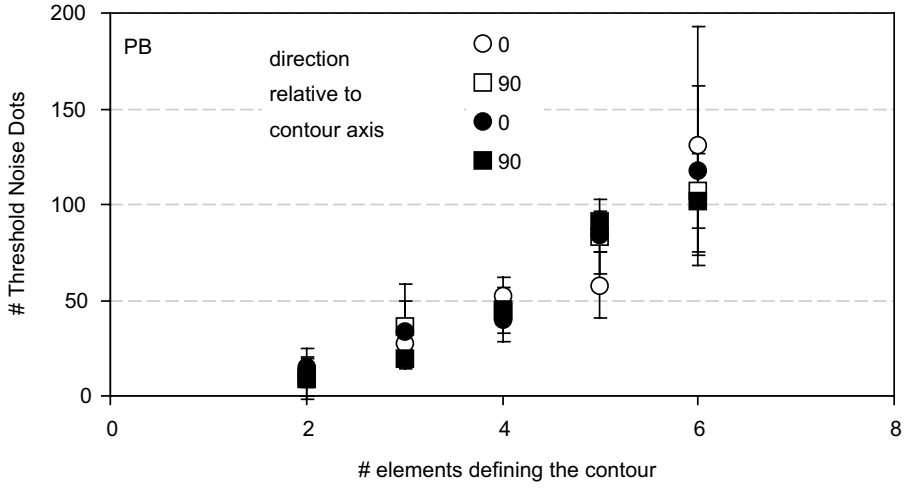

Fig. 9. Visibility of a contour as a function of the number of elements and direction of motion of the contour. As Fig. 4, except that the elements defining the contour were dark (<1 cd/m^2, filled symbols) or white (100 cd/m^2, open symbols) Gaussian ($\sigma = 2$ arcmin) dots and moved rigidly at 0 deg (circles) or 90 deg (squares) relative to the contour axis. Noise elements moved in a direction randomly assigned at the start of the trial.

observer will detect the coherent motion of any of the target elements of a parallel contour without necessarily detecting the contour structure itself.

With quite different stimuli and tasks (random noise drifting within static Gaussian windows and per cent correct detection measured with eight target elements and a fixed number of noise elements), Ledgeway and Hess (2002) reported that non-rigid contours were more visible than rigid contours of low curvature. At contour curvature greater than 20 deg, rigid contours were in some cases more visible than non-rigid ones (their Fig. 2). Most of our data were collected with contours of 20 deg or greater curvature and show no systematic directional effects and are consistent with their results. However, we found no reliable effect of direction for straight contours ($\alpha = 0$ deg), where the largest difference occurred in their data. Note that for straight contours, there is no difference between rigid and non-rigid contours in either study (because all elements move toward the next one), so there can be no difference in their

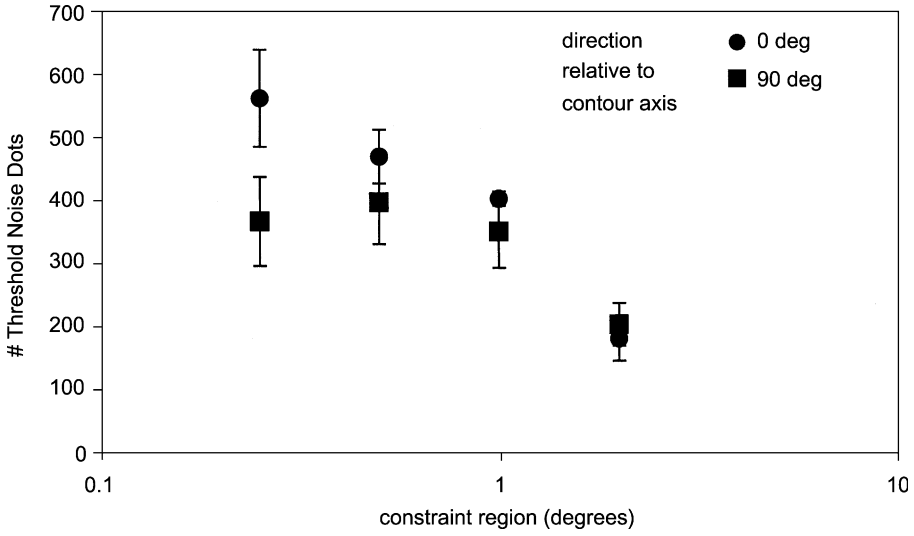

Fig. 10. Visibility of a three element contour in random walk noise as a function of its direction of motion and its proximity to central visual field. The elements defining the contour were dark (<1 cd/m^2) Gaussian ($\sigma = 2$ arcmin) dots that moved rigidly at 0 deg (circles) or 90 deg (squares) relative to the contour axis. The centre element of the triplet was constrained to pass within 0.25–2 deg of fixation, as indicated by the x-axis. Noise elements moved in a direction randomly assigned each animation frame. Data points are the mean of the three observers, error bars show ±1 s.e.m. None of the observers differed from this pattern.

visibility under these conditions. We therefore speculate that the difference between studies may depend on differences in the randomisation of element direction in the studies. While we measured only principal directions (0, 45 and 90 deg), they randomised the direction of the elements relative to the path orientation in their rigid contours, this additional source of uncertainty may account for the lower visibility of non-parallel contours.

6.2. Spatial frequency and contrast polarity in contour grouping

All the data were collected with band-pass elements with peak spatial frequencies at 1.5, 3 or 6 c/deg but the results were strikingly similar in all conditions. For static images composed of oriented Gabor micro-patterns with constant standard deviation (envelope size) performance is also invariant of spatial frequency over this range (Dakin & Hess, 1998a, 1998b), although the visibility of static contours decreases with separation when expressed as multiples of the carrier frequency of the Gabor micro-pattern (Kovacs & Julesz, 1993). When the spatial frequency of alternating elements varies, Dakin and Hess (1998a, 1998b) report bandwidths that vary with the curvature of the contour: bandwidths vary from 2.6 octaves at $\alpha = 0$ deg to 1.4 octaves at $\alpha = 30$ deg, and are 1.76 where $\alpha = 20$ deg (mean of their observers). The bandwidth measured here with moving contours are somewhat larger at 2.53 octaves, where $\alpha = 20$ deg. With motion coherence tasks based on band-pass filtered dots similar to those employed here, we have recently estimated the bandwidth of local motion detectors at approximately 1 octave (Bex & Dakin, 2002), which is somewhat lower than the present estimate of bandwidth for contour grouping. In that study we also measured the bandwidth of grouping processes for global patterns of motion (translation, rotation and expansion/contraction) and found them to be extremely broadly tuned (>3 octaves) when the visibility of the elements was equated, as in the present study.

We also found that contours composed of elements of alternating contrast polarity were as visible as those composed of elements of the same contrast polarity. In global motion coherence tasks, Edwards and Badcock (1994) reported that while elements of opposite contrast polarity were not integrated in local motion detection, they were integrated for global motion tasks because positive and negative polarity elements were equally effective at masking a global motion signal carried by either positive and negative polarity elements. Our results are consistent with their interpretation that motion integration processes combine motion signals carried by ON and OFF pathways. Therefore the present results share some of the properties (broad tuning for spatial frequency and indifference to contrast polarity) that have been observed elsewhere for global motion detection.

6.3. Contour integration or detection of pockets of high signal to noise ratio?

The distribution of directions in the interval containing the contour is biased by the uniform directions of the contour elements. Therefore one of the simplest explanations of our results might be that observers choose the interval containing this biased directional distribution. This strategy would be effective for an ideal

observer and would not require any contour-linking at all. If this were true, we would expect the number of threshold noise elements to increase with Weber's law as the number of target elements increases. The results of Experiment 1 (Fig. 4), showing that detection thresholds as a function of the number of contour elements are well-fit by a constant Weber fraction (14% across observers) are consistent with this simple interpretation.

However, we also found (Fig. 6) that reducing the spacing between elements improved their visibility even though this does not affect the overall distribution of directions. But, one only has to allow the averaging process to operate over a spatially-restricted region of the display (i.e. a small area of relatively high signal:noise ratio) to account for these effects with a simple model based on the distribution of directions. Any explanation based on locally high signal to noise ratios predicts that performance should slightly *increase* with curvature because the geometric separation among elements decreases as curvature increases (i.e. the mean distance between elements is greater for straight than highly curved paths). However, the results in Fig. 7 show a modest *decrease* in contour visibility at high curvature.

Simple averaging also dictates that non-rigid contours should be less visible than rigid ones because non-rigid contours contain a broader distribution of directions, especially for highly curved contours. However, the results are the same for rigid and non-rigid paths across all conditions (filled symbols, PB all figures).

Taken together, our results militate against simple directional averaging and show that the visibility of moving contours is determined by the shape that is defined by the directions of the elements forming the contour.

Acknowledgements

PJB was supported by the Welcome Trust and by BSRC, AJS was supported by the MRC, SCD was supported by BBSRC.

A preliminary report of these data was presented at the second annual meeting of the Vision Sciences Society (Bex, Simmers, & Dakin, 2002).

References

Beaudot, W. H. A. (2002). Role of onset asynchrony in contour integration. *Vision Research, 42*(1), 1–9.

Bex, P. J., & Dakin, S. C. (2002). Comparison of the spatial-frequency selectivity of local and global motion detectors. *Journal of the Optical Society of America A—Optics Image Science and Vision, 19*(4), 670–677.

Bex, P. J., Simmers, A. J., & Dakin, S. C. (2001). Snakes and ladders: the role of temporal modulation in visual contour integration. *Vision Research, 41*(27), 3775–3782.

Bex, P. J., Simmers, A. J., & Dakin, S. C. (2002). Integration of moving contours from local directional signals. *Journal of Vision, 2*(7), 655a.

Dakin, S. C., & Bex, P. J. (2002). Role of synchrony in contour binding: some transient doubts sustained. *Journal of the Optical Society of America A, 19*(4), 678–686.

Dakin, S. C., & Hess, R. F. (1998a). Spatial-frequency tuning of visual contour integration. *Journal of the Optical Society of America, A, 15*(6), 1486–1499.

Dakin, S. C., & Hess, R. F. (1998b). The spatial-frequency tuning of visual contour integration. *Perception, 27*(2), 14.

Dakin, S. C., & Hess, R. F. (1999). Contour integration and scale combination processes in visual edge detection. *Spatial Vision, 12*(3), 309–327.

Devalois, R. L., & Devalois, K. K. (1991). Vernier acuity with stationary moving gabors. *Vision Research, 31*(9), 1619–1626.

Edwards, M., & Badcock, D. R. (1994). Global motion perception—interaction of the on and off pathways. *Vision Research, 34*(21), 2849–2858.

Farid, H., & Adelson, E. H. (2001). Synchrony does not promote grouping in temporally structured displays. *Nature Neuroscience, 4*(9), 875–876.

Field, D. J., Hayes, A., & Hess, R. F. (1993). Contour integration by the human visual system: evidence for a local "association field". *Vision Research, 33*(2), 173–193.

Hayes, A. (2000). Apparent position governs contour-element binding by the visual system. *Proceedings of the Royal Society of London Series B, 267*(1450), 1341–1345.

Hess, R. F., & Dakin, S. C. (1997). Absence of contour linking in peripheral vision. *Nature, 390*(6660), 602–604.

Hess, R. F., & Dakin, S. C. (1999). Contour integration in the peripheral field. *Vision Research, 39*(5), 947–959.

Hess, R. F., & Field, D. J. (1995). Contour integration across depth. *Vision Research, 35*(12), 1699–1711.

Hess, R. F., Hayes, A., & Kingdom, F. A. (1997). Integrating contours within and through depth. *Vision Research, 37*(6), 691–696.

Keeble, D. R. T., & Hess, R. F. (1999). Discriminating local continuity in curved figures. *Vision Research, 39*(19), 3287–3299.

Kovacs, I., & Julesz, B. (1993). A closed curve is much more than an incomplete one: effect of closure in figure-ground segmentation. *Proceedings of the National Academy of Science, 90*, 7495–7497.

Ledgeway, T., & Hess, R. F. (2002). Rules for combining the outputs of local motion detectors to define simple contours. *Vision Research, 42*(5), 653–659.

Lee, S. H., & Blake, R. (1999). Visual form created solely from temporal structure. *Science, 284*(5417), 1165–1168.

Morgan, M., & Castet, E. (2002). High temporal frequency synchrony is insufficient for perceptual grouping. *Proceedings of the Royal Society of London Series B, 269*(1490), 513–516.

Moulden, B. (1994). Collator units: second stage orientational filters. In R. Bock (Ed.), *Higher order processing in the visual system*. New York, NY: John Wiley.

Moulden, B., Kingdom, F. A., & Gatley, L. F. (1990). The standard deviation of luminance as a metric for contrast in random-dot images. *Perception, 19*(1), 79–101.

Mullen, K., Beaudot, W. H. A., & McIlhagga, W. H. (2000). Contour integration in color vision: a common process for the blue–yellow, red–green and luminance mechanisms? *Vision Research, 40*(6), 639–655.

Pelli, D. G. (1997). The VideoToolbox software for visual psychophysics: Transforming numbers into movies. *Spatial Vision, 10*, 437–442.

Pelli, D. G., & Zhang, L. (1991). Accurate control of contrast on microcomputer displays. *Vision Research, 31*(7–8), 1337–1350.

Pettet, M. W. (1999). Shape and contour detection. *Vision Research, 39*(3), 551–557.

Press, W. H., Teukolsky, A. A., Vetterling, W. T., & Flannery, B. P. (1992). *Numerical recipes in C*. Cambridge, England: Cambridge University Press.

Roelfsema, P. R., Scholte, H. S., & Spekreijse, H. (1999). Temporal constraints on the grouping of contour segments into spatially extended objects. *Vision Research, 39*(8), 1509–1529.

Usher, M., & Donnelly, N. (1998). Visual synchrony affects binding and segmentation in perception. *Nature, 394*(6689), 179–182.

Verghese, P., McKee, S. P., & Grzywacz, N. M. (2000). Stimulus configuration determines the detectability of motion signals in noise. *Journal of the Optical Society of America A, 17*(9), 1525–1534.

Watamaniuk, S. N., McKee, S. P., & Grzywacz, N. M. (1995). Detecting a trajectory embedded in random-direction motion noise. *Vision Research, 35*(1), 65–77.

Watson, A. B., & Pelli, D. G. (1983). QUEST: A Bayesian adaptive psychometric method. *Perception and Psychophysics, 33*, 113–120.